The final publication is available at

http://doi.org/10.1016/j.ins.2008.06.010

Additional Information

A new graphical visualization of n-dimensional Pareto front for decision-making in multiobjective optimization

X. Blasco [a,*] J.M. Herrero [a] J. Sanchis [a] M. Martínez [a]

[a] *Predictive Control and Heuristic Optimization Group*

Department of Systems Engineering and Control

Universidad Politécnica de Valencia.

Camino de Vera S/N, 46022-Valencia, Spain.

Abstract

New challenges in engineering design lead to multiobjective (multicriteria) problems. In this context, the Pareto front supplies a set of solutions where the designer (decision-maker) has to look for the best choice according to his preferences. Visualization techniques often play a key role in helping decision-makers, but they have important restrictions for more than two-dimensional Pareto fronts. In this work, a new graphical representation, called *Level Diagrams*, for n-dimensional Pareto front analysis is proposed. *Level Diagrams* consists of representing each objective and design parameter on separate diagrams. This new technique is based on two key points: classification of Pareto front points according to their proximity to ideal points measured with a specific norm of normalized objectives (several norms can be used); and synchronization of objective and parameter diagrams. Some of the new possibilities for analyzing Pareto fronts are shown. Additionally, in order to introduce designer preferences, Level Diagrams can be coloured, so establishing a visual representation of preferences that can help the decision-maker. Finally, an example of a robust control design is presented - a benchmark proposed at the American Control Conference. This design is set as a six-dimensional multiobjective problem.

Key words: multiobjective optimization, multidimensional visualization, decision making tools, high dimensional Pareto front

* Corresponding author. DISA-Universidad Politécnica de Valencia.

Camino de Vera S/N, 46022-Valencia, Spain.
  Email address: xblasco@isa.upv.es (X. Blasco).
  URL: ctl-predictivo.upv.es (X. Blasco).

2

1 Motivation

In numerous engineering areas, the task of obtaining suitable designs becomes a multiobjective (or multicriteria) problem. This means it is necessary to look for a solution in the design space that satisfies several specifications (objectives) in the performance space. Generally, these specifications are conflicting, that is, there is no simultaneous optimal solution for all of them. In this context, the solution is not unique, instead there is a set of possible solutions where none is best for all objectives. This set of optimal solutions in the design space is called the Pareto set. The region defined by the performances (the value of all objectives) for all Pareto set points is called the Pareto front.

The exact determination of the Pareto front is unrealistic for real-world problems, as it is usually an infinite set. Therefore, it is usual to focus on obtaining a discrete approximation. A common step for solving a multiobjective optimization problem is to obtain the discrete approximation of the Pareto front. This is an open research field where numerous techniques have already been developed [19] and where new techniques are being constantly developed [17,14]. An alternative, and very active research line, is Multiobjective Evolutionary Algorithms [5,9]. In general, these algorithms supply reasonable solutions for Pareto front approximations. Once obtained, the next step for the designer is to select one, or more, solutions inside the Pareto front approximation. The final solution is often selected using methodologies that normally include designer preferences. Different approaches to introducing preferences can be found in the literature [19,4,25]. The usual classification is based on when the Decision Maker (DM) is consulted: a priori, a posteriori, and progressive (or interactive) decision; and the DM has to introduce preferences before, after,

or during the optimization process respectively.

Decision-making techniques (decision support systems), or simply tools for helping decision-makers, is a field in constant development with interesting and successful solutions in:

- A priori methodology [16].
- Progressive methodology [22].
- A posteriori methodologies [7,23,6,21,26,13,12].

It is widely accepted that visualization tools are valuable and provide decision-makers with a meaningful method to analyze the Pareto set and select good solutions. For two-dimensional problems (and sometimes for three-dimensional) it is usually straightforward to make an accurate graphical analysis of the Pareto set point possibilities, but this becomes more difficult for higher dimensions. Several of the techniques proposed for multidimensional visualization can be consulted at [2]. The most common are:

- Scatter diagrams: The visualization consists of an array of scatter diagrams arranged in the form of an n x n matrix. Each dimension of the original data defines one row and column of the matrix. The complexity of the representation increases notably with the dimension.
- Parallel coordinates: A multidimensional point is plotted in a two-dimensional graph. Each dimension of original data is translated to an x coordinate in the two-dimensional plot. This is a very compact way of presenting multi-dimensional information, but with large sets of data it loses clarity and the analysis becomes difficult to perform.

Other more complex, but interesting, alternatives offering graphical represen-

50 tation can be consulted at [1,24,11,27].

51 This work contributes a new alternative, called *Level Diagrams*. It enables
52 easier analysis of the Pareto set (and Pareto set approximations supplied by
53 multiobjective optimization techniques) and so may become a useful tool for
54 decision-makers. *Level diagrams* can be used in an a priori and progressive
55 methodology to help the DM. *Level Diagrams* tries to be a *geometrical* visu-
56 alization of the Pareto front and set, which when combined with a colouring
57 methodology of the points based on preferences, can be a powerful tool to help
58 DM's make decisions.

59 The following sections describe the proposed graphical representation and
60 show simple examples. Subsequently, this representation is used in a more
61 complex problem that involves choosing an adequate solution to a multiobjec-
62 tive problem with six dimensions in performance space and six dimensions in
63 parameter space. Additionally, a method to show designer preferences in the
64 *Level Diagrams* is enabled by colouring the points.

65 ## 2 Level Diagrams for Pareto front

66 Multiobjective problems can be formalized as follows:

$$
\begin{aligned}
\theta &= [\theta_1, \ldots, \theta_l] \in \mathcal{D} \\
\mathbf{J}(\theta) &= [J_1(\theta), \ldots, J_s(\theta)] \\
&\min_{\theta \in \mathcal{D}} \mathbf{J}(\theta)
\end{aligned}
\tag{1}
$$

67 where θ is the decision vector, $\mathcal{D}$ is the decision space, and $\mathbf{J}(\theta)$ is the objective
68 vector.

Without loss of generality, a multiobjective minimization problem is considered [1] . This involves the simultaneous minimization of all objectives $J_i(\theta)$. In general, there is no single solution: in fact, there is a set of solutions where none is better than others. Using a definition of *dominance*, the Pareto set $\mathbf{\Theta}_p$ is the set of every non-dominated solution. Pareto dominance is defined as follows.

A solution θ^1 dominates another solution θ^2, denoted by $\theta^1 \prec \theta^2$, if

$$\forall i \in \{1, \ldots, s\}, J_i(\theta^1) \leq J_i(\theta^2) \ \wedge \ \exists k \in \{1, \ldots, s\} : J_k(\theta^1) < J_k(\theta^2) \qquad (2)$$

Therefore, the Pareto optimal set $\mathbf{\Theta}_P$, given by

$$\mathbf{\Theta}_P = \{\theta \in D \mid \nexists \ \tilde{\theta} \in D \ : \ \tilde{\theta} \prec \theta\} . \qquad (3)$$

$\mathbf{\Theta}_P$ is unique, and normally includes infinite solutions. Hence, a set $\mathbf{\Theta}_P^*$, with a finite number of elements from $\mathbf{\Theta}_P$, should be obtainable [2] , and this should be the goal of multiobjective algorithms. In fact, the realistic goal of a multiobjective algorithms is to obtain a discrete approximation of the Pareto front. In the following, this discrete approximation is referenced as $\mathbf{\Theta}_P^*$.

At this point, the decision-maker has a set $\mathbf{\Theta}_p^* \subset \mathcal{R}^l$, that constitutes the Pareto set discrete approximation and an associated set of objective values for every point that constitutes an approximation to the Pareto front $\mathbf{J}(\mathbf{\Theta}_p^*) \subset \mathcal{R}^s$.

The *Level Diagrams* tool is based on the classification of the Pareto front

---

[1] A maximization problem can be easily converted to a minimization problem, for instance for each one of the objectives that have to be maximized, the following transformation could be applied: $\max J_i(\theta) = -\min(-J_i(\theta))$

[2] Notice that $\mathbf{\Theta}_P^*$ is not unique.

6

88 approximation $(\mathbf{J}(\boldsymbol{\Theta}_p^*))$ according to the proximity to the ideal point[3].

89 For this classification, every objective $(J_i(\theta), i = 1 \dots s)$ is normalized with re-

90 spect to its minimum and maximum values on the Pareto front approximation,

91 $\bar{J}_i(\theta), i = 1 \dots s$:

$$J_i^M = \max_{\theta \in \boldsymbol{\Theta}_p^*} J_i(\theta); \; J_i^m = \min_{\theta \in \boldsymbol{\Theta}_p^*} J_i(\theta); \; i = 1 \dots s \tag{4}$$

$$\bar{J}_i(\theta) = \frac{J_i(\theta) - J_i^m}{J_i^M - J_i^m} \rightarrow 0 \leq \bar{J}_i(\theta) \leq 1 \tag{5}$$

94 A norm is applied to evaluate the distance to the ideal point. Different norms

95 could be used to obtain different characteristics of the diagrams, the most

96 common being:

97 • 1-norm: $||\bar{\mathbf{J}}(\theta)||_1 = \sum_{i=1}^{s} |\bar{J}_i(\theta)|$

98 • Euclidean norm (2-norm): $||\bar{\mathbf{J}}(\theta)||_2 = \sqrt{\sum_{i=1}^{s} \bar{J}_i(\theta)^2}$

99 • Infinite norm (∞-norm): $||\bar{\mathbf{J}}(\theta)||_\infty = \max\{\bar{J}_i(\theta)\}$

100 Depending on the selected norm and the dimension of the objective vector,

101 the value for each is:

$$0 \leq ||\bar{\mathbf{J}}(\theta)||_1 \leq s \tag{6}$$
$$0 \leq ||\bar{\mathbf{J}}(\theta)||_2 \leq \sqrt{s} \tag{7}$$
$$0 \leq ||\bar{\mathbf{J}}(\theta)||_\infty \leq 1 \tag{8}$$

102 Each norm gives a different point of view of the Pareto front shape, for in-

103 stance:

104 • Euclidean norms supply an accurate evaluation of the conventional geomet-

---

[3] The ideal point [19] is a point with the minimum value of the Pareto front at each objective.

7

105 rical distance to the ideal point, and then offer a better view of the '*real*'
106 shape.

107 • ∞-norm can supply information about the worst objective for a specific
108 point, and is useful for trade-off analysis between different objectives. An
109 increment in this norm directly reveals a worsening of at least one of the
110 objectives. The use of ∞-norm is the generalization of the representation
111 by layers described at [3].

112 To plot *Level Diagrams*, the points of the Pareto front are sorted in ascending
113 order of the value of the $||\bar{\mathbf{J}}(\theta)||_x$. Once every point is classified, the graphical
114 representation of the Pareto front, and the Pareto set, is performed with the
115 following methodology. Each objective (J_i) and decision variable (θ_j) has its
116 own graphical representation. Axis Y on all the graphs corresponds to the value
117 of $||\bar{\mathbf{J}}(\theta)||_x$, and this means that all graphs are synchronized with respect to
118 this axis. Axis X corresponds to values of the objective, or decision variables,
119 in physical units.

120 It is important to remark that for an adequate interpretation of *Level Dia-*
121 *grams*, each objective and component of a point is represented at the same
122 Y position (level) for all graphs, and this means all information for a single
123 point is drawn at the same position on the Y axis for all graphs J_i and θ_j.

124 The following simple example of *Level Diagrams* is shown to clarify this new
125 alternative. A classical 2D problem is selected, although *Level Diagrams* is not
126 necessary for a 2D problem (classical representation is sufficient).

127 Characteristics of the multiobjective problem 1 (MOP1) are:

$$-10^5 \le \theta \le 10^5,$$

8

$$J_1(\theta) = \theta^2, \tag{9}$$
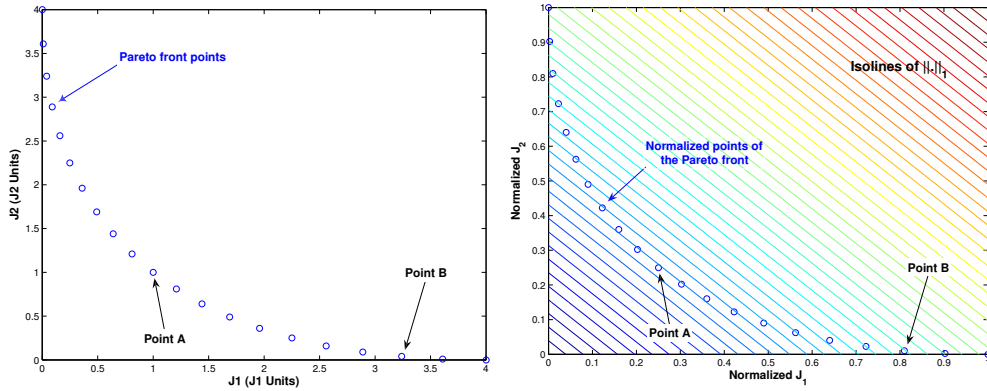$$J_2(\theta) = (\theta - 2)^2, \tag{10}$$

Fig. 1. Pareto front classical 2D representation of Θ_P^* for MOP1. Normalized 2D representation with isolines for 1-Norm.
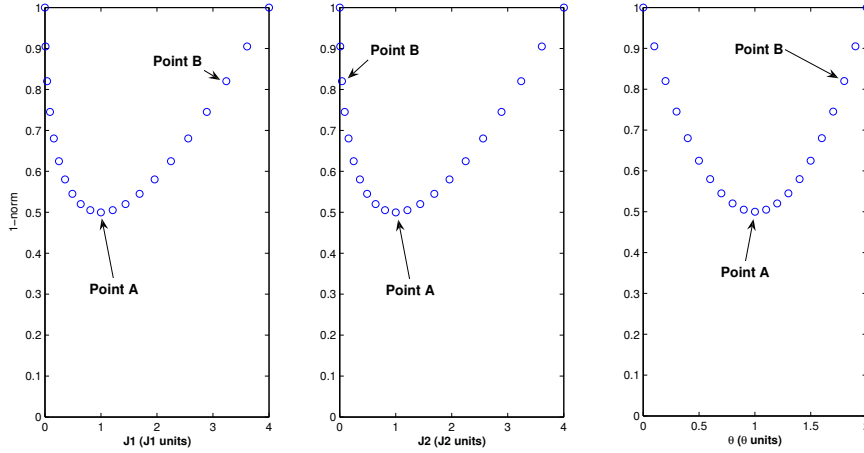

Fig. 2. 1-norm *Level Diagrams* representation for MOP1 problem.

Figures 1 and 2 show a 2D classical representation and *Level Diagrams* respectively [4] for a discrete set of Pareto points of the MOP1 problem. Figure 1

---

[4] Objective and parameter axes with a physical meaning are marked with Ji (Ji Units) and θ (θ Units) respectively. For a real problem, these 'Units' have a specific meaning and offer a real meaningfulness that gives valuable information to the designer.

9

shows the most common type of representation of a 2D Pareto front[5]. Isolines of 1-norm on the the same figure are shown.

Each point of the Pareto front $\mathbf{J}(\boldsymbol{\Theta}_p^*)$ corresponds to a point on each graph (J_1 and J_2) on *Level Diagrams* (see figure 2). For instance, point A at figure 1 corresponds to points A on all graphs (J_1, J_2) of figure 2, point B of figure 1 corresponds to points B in figure 2, etc.

The Pareto set $\boldsymbol{\Theta}_p^*$ is drawn in a similar way. The classification of the Pareto front points is maintained, and then for each component of a Pareto set there is an associated graph. A point is drawn at the same level (Y coordinate) on each graph and this level is the same for the associated Pareto front point (see graph θ at figure 2).

In the *Level Diagram* representation, point A of the Pareto front of figure 1 is represented with three points in figure 2. One point is shown in the J_1 graph, one point in the J_2 graph, and another in the θ graph. All these points are at the same position on the Y axis, and this position shows the distance to the ideal point with a particular norm, (in the example, 1-norm).

3   Pareto front graphical analysis

The proposed graphical representation enables a new analysis of large sets of Pareto points (or Pareto point approximation obtained from a multiobjective optimization algorithm). Pareto fronts and sets can also be analyzed simultaneously. This new alternative gives the DM valuable information about the

---

[5] Each objective on one axis. This type of representation is only possible for 2D and 3D cases.

characteristics of the different zones of the Pareto front. Remember, that all points of the Pareto front are optimum in some sense, and could be useful for different design alternatives depending on DM preferences. Some of the characteristics that can be analyzed are:

- The points situated at the lower levels corresponding to the zones of the Pareto front nearer to the ideal point.
- Qualitative analysis of Pareto front or set discontinuities: these are visible when a vertical band at *Level Diagrams* is empty, or when there are discontinuities in the norm axes. These empty bands give an unreachable range of values for the objective function and parameter design. Remember, that X axes are represented in physical units, so the DM can quickly obtain an unreachable range in physical units.
- Analysis of trade-off between several objectives.

Two simple examples are presented to show the use of this visualization. Both examples correspond to typical test functions in multiobjective literature.

3.1   Test problem MOP2

This test problem has the following characteristics: both Pareto front and set are bi-dimensional and discontinuous. Functions to optimize are $\mathbf{J}(\theta) = [J_1(\theta), J_2(\theta)]$, $\theta = [\theta_1, \theta_2]$ where:

$$J_1(\theta) = \left(1 + (A_1 - B_1)^2 + (A_2 - B_2)^2\right), \tag{11}$$
$$J_2(\theta) = (\theta_1 + 3)^3 + (\theta_2 + 1)^2, \tag{12}$$

$$A_1 = 0.5\sin(\theta_1) - 2\cos(\theta_1) + \sin(\theta_2) - 1.5\cos(\theta_2),$$
$$A_2 = 1.5\sin(\theta_1) - \cos(\theta_1) + 2\sin(\theta_2) - 0.5\cos(\theta_2),$$

11

$$B_1 = 0.5\sin(\theta_1) - 2\cos(\theta_1) + \sin(\theta_2) - 1.5\cos(\theta_2),$$

$$B_2 = 1.5\sin(\theta_1) - \cos(\theta_1) + 2\sin(\theta_2) - 0.5\cos(\theta_2),$$

$$-\pi \leq \theta_1 \leq \pi; \quad -\pi \leq \theta_2 \leq \pi.$$

170 For the MOP2 problem, the multiobjective evolutive algorithm ϵ-MOGA [6]

171 gives 868 points as the Pareto front approximation. The graphics in figure 3

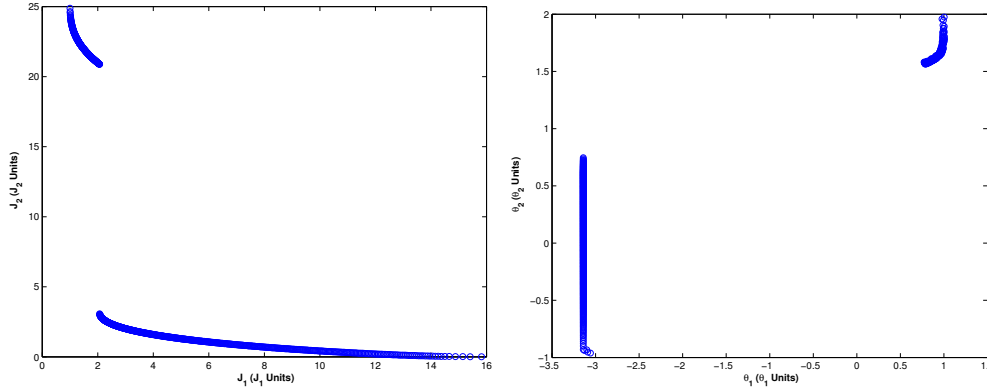172 are obtained with the classical representation.

Fig. 3. Classical representation of Pareto front and set for the MOP3 problem.

173 The graph shown in figure 4 is obtained with the new representation.

174 For this problem, the principal characteristics of the Pareto front and set can

175 be observed with both visual representations - classical and *Level Diagrams*.

176 Let's analyze the Pareto front first:

[6] The ϵ-MOGA variable (ϵ-MOGA) [8,10] is an elitist multiobjective evolutionary algorithm based on the concept of ϵ-dominance [20]. ϵ-MOGA obtains an ϵ-Pareto set, Θ_P^*, that converges towards the Pareto optimal set Θ_P in a distributed manner around Pareto front $\mathbf{J}(\Theta_P)$, with limited memory resources. It also dynamically adjusts the limits of the Pareto front $\mathbf{J}(\Theta_P^*)$ and avoids losing the Pareto front extremities.
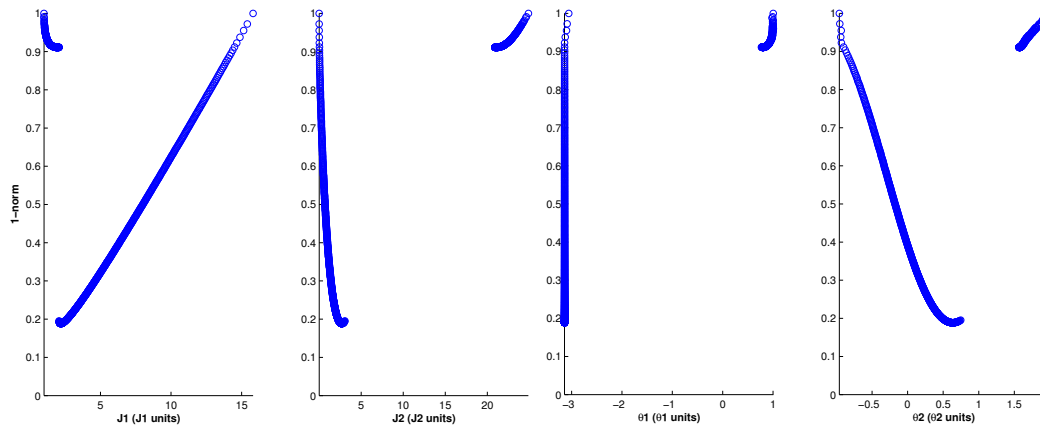
12

Fig. 4. 1-norm *Level Diagrams* representation of Pareto front and set approximation for the MOP3 problem.

- The whole range of J_1 between the maximum and minimum can be reached by points of the Pareto front. This does not happen for J_2 where there are unreachable values of the Pareto front (approximately between 4 and 21). This means there are discontinuities along the front (or at least along its discrete approximation).

- There are points near the ideal point and so it is relatively simple for the designer (or DM) to choose a unique solution.

- It is quite simple to maintain a low value of J_2, but if a value of $J_1 < 2$ is required then J_2 has to be greatly increased.

In a similar way, the Pareto set can be analyzed:

- Values of the Pareto set are localized at two particular zones: $\theta_1 \approx -3.1$, $\theta_2 \in [-1, 0.75]$ and $\theta_1 \in [0.8, 1]$, $\theta_2 \in [1.55, 2]$. Notice that there are discontinuities in the Pareto set.

With the new visual representation, it is possible to view the same characteristics, and the precision of the range of values is probably improved because the Pareto front and set are better related to the physical unit range. For

13

¹⁹³ instance, it is easier to see the range value of the nearest point to the ideal

¹⁹⁴ point: $\theta_1 \approx -3.1$, $\theta_2 \approx 0.5$. In the classical representation, the Pareto set and

¹⁹⁵ Pareto front are unsynchronized.

3.2 Test problem MOP3

¹⁹⁶

¹⁹⁷ Although the new visual representation could seem less intuitive than the

¹⁹⁸ classical view for bi-dimensional problems, it offers huge possibilities as the

¹⁹⁹ dimension of the optimization problem grows because it enables a graphical

²⁰⁰ analysis that is very difficult to achieve with other methods.

²⁰¹ The MOP3 test problem is not yet a very high dimensional problem, but

²⁰² presents some characteristics that complicate analysis in the classical way. The

²⁰³ MOP3 problem has the following characteristics: the Pareto front is a line in

²⁰⁴ the three-dimensional objective space, and the Pareto set is bi-dimensional

²⁰⁵ and discontinuous.

²⁰⁶ Functions to minimize are $\mathbf{J}(\theta) = [J_1(\theta), J_2(\theta), J_3(\theta)]$, $\theta = [\theta_1, \theta_2]$ where:

$$J_1(\theta) = 0.5(\theta_1^2 + \theta_2^2) + \sin(\theta_1^2 + \theta_2^2), \tag{13}$$

$$J_2(\theta) = \frac{(3\theta_1 - 2\theta_2 + 4)^2}{8} + \frac{(\theta_1 - \theta_2 + 1)^2}{27}, \tag{14}$$

$$J_3(\theta) = \frac{1}{(\theta_1^2 + \theta_2^2 + 1)} - 1.1e^{(-\theta_1^2 - \theta_2^2)} + 0.2, \tag{15}$$

$$-3 \leq \theta_1 \leq 3; \quad -3 \leq \theta_2 \leq 3.$$

²⁰⁷ The approximation to the Pareto front is obtained with $\not\!{\varepsilon}$MOGA and has 775

²⁰⁸ points. The 3D visual representation is shown in figure 5. As can be seen, it is

²⁰⁹ very difficult to obtain useful conclusions about the principal characteristics

²¹⁰ of the Pareto front; and it is difficult to obtain range values for each objective.

14

211 It is also very difficult to see the nearest zone to the ideal point, and it is not
212 clear if there are discontinuities, etc.

213 Other common alternatives for graphical representation are:

214 • **Parallel coordinates**. Each objective is represented in a vertical axis as
215 shown in figure 6. However, when the Pareto front is described with a large
216 number of points, then interpretation with this visual technique becomes
217 very complicated.

218 • **Scatter plot**. Consists in the projection of all the pairs of objectives as
219 shown in figure 7. In this case, analysis is difficult.

220 In both cases, the Pareto front and Pareto set could be synchronized by draw-
221 ing each point with different colours, but this method is less direct than the
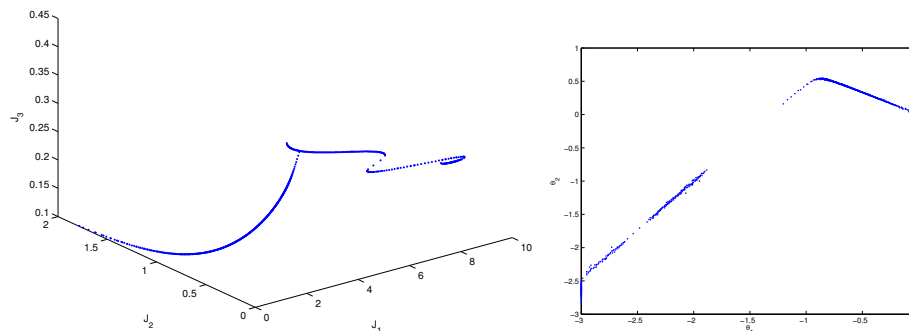222 synchronization performed in *Level Diagrams*.

Fig. 5. Classical representation of the Pareto front and set for the MPO3 problem.

223 Figure 8 shows the *Level Diagrams* representation for the MPO3 Pareto solu-
224 tion. Some interesting conclusions, that may help the DM, can be made:

225 • It is a Pareto front with numerous points at the lower levels, and that means
226 there are numerous points relatively close to the ideal point. Therefore, it
227 is a front where a reasonable compromise between objectives can be found.
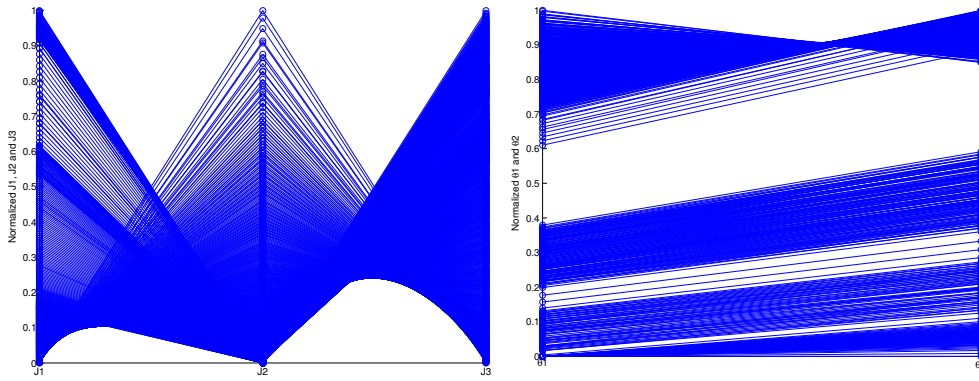
15

Fig. 6. Parallel coordinate (with normalized axes) representation of Pareto front and set for the MPO3 problem.
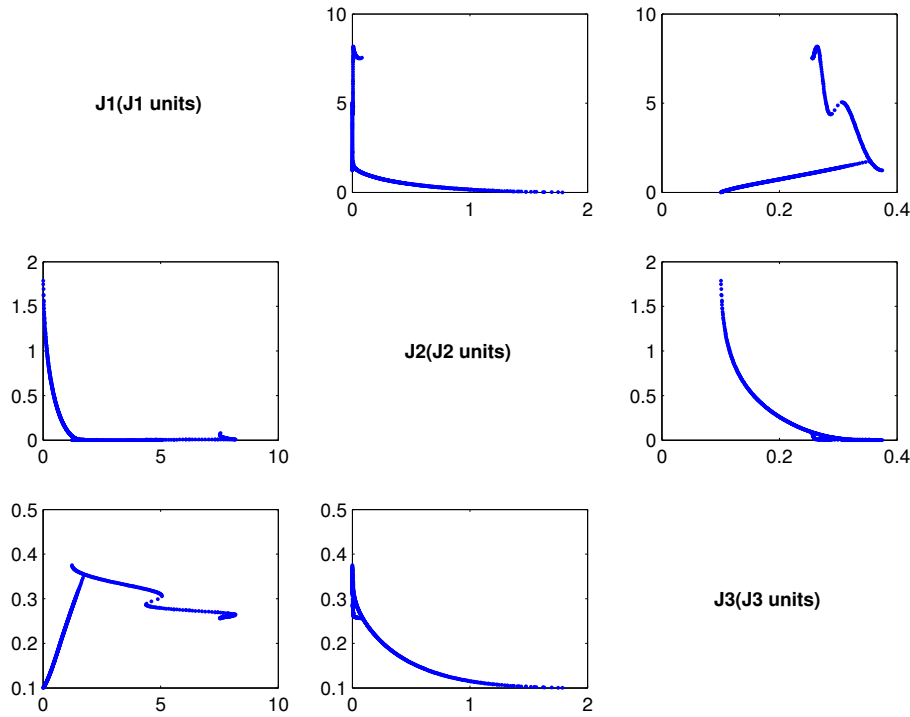

Fig. 7. Scatter plot representation of Pareto set for MOP3 problem.

228 • The nearest points to the ideal are at: $J_1 \in [0.4, 0.6]$, $J_2 \in [0.35, 0.55]$ and

229   $J_3 \in [0.15, 0.18]$. These values mark the order of magnitude for an adequate

230   compromise between all objectives.

231 • A similar analysis could be made with the Pareto set. The values of the front

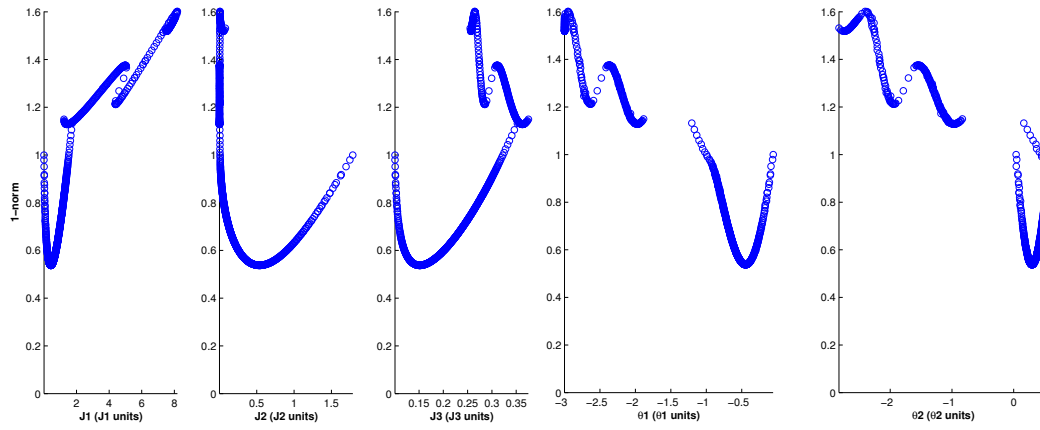232   nearest to the ideal point, have the following range of values: $\theta_1 \approx -0.5$,

16

Fig. 8. 1-norm *Level Diagrams* representation of the Pareto set and front for the MPO3 problem.

233 $\theta_2 \approx 0.3$.

234 • If the Pareto front has no discontinuities at any of the objectives, then all

235   values inside the range of the Pareto front can be achieved for each objective

236   separately. If required by the DM, a specific value of one objective function

237   can always be obtained and it is optimum in the Pareto sense. For instance, if

238   the designer thinks that $J_1(\theta)$ has to be in the range $[2, 4]$, after seeing *Level*

239   *Diagrams*, then it is necessary to choose a point of 1-norm in range $[1.2, 1.35]$.

240   At this level, the other objectives and design parameters are situated at the

241   ranges: $J_2(\theta) \approx 0, 0.3 \leq J_3(\theta) \leq 0.35, -2.5 \leq \theta_1 \leq -2$ and $-1.7 \leq \theta_2 \leq -1$.

242   Qualitatively, J_2 is improved and J_3 is worsened - compared with the zone

243   nearest to the ideal point. The design parameters are in a zone clearly

244   different from the one nearest to the ideal point. Therefore, the designer

245   can have an idea of the value for each objective and design parameter.

246 • A discontinuity can be observed in the design parameters. There is a a gap

247   in the ranges: $-2 \leq \theta_1 \leq -1.5$ and $-1 \leq \theta_2 \leq -0.2$.

17

4   Application example for a six-dimensional problem

249 To illustrate the *Level Diagrams* utility, a multiobjective design of a controller

250 is described. The problem is based on a robust control benchmark proposed

251 at the American Control Conference (ACC). Wie and Bernstein [28] proposed

252 a series of problems for robust control - in which the controller designer must

253 achieve a trade-off between maximizing stability and robust system perfor-
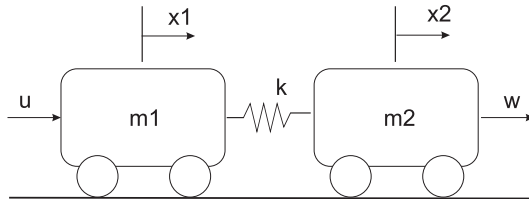
254 mance, and minimizing control effort.

Fig. 9. A two mass and spring system with uncertainties in the parameters.

255 Figure 9 shows the process described in the benchmark. It is a flexible structure

256 of two masses connected by a spring. x_1 and x_2 indicate mass 1 and mass

257 2 positions. The nominal values for the two masses and for the spring are

258 $m_1 = m_2 = k = 1$. Control action u is the strength applied to mass 1, and

259 controlled variable y is the mass 2 position x_2 affected by noise measurements

260 v. Moreover, there is a disturbance w on mass 2.

261 *4.1   Design objectives*

262 The specific problem is to obtain a coefficient of the controller transfer function

263 with six degrees of freedom. The numerator and denominator coefficients give

264 the parameter vector to be obtained by optimization $\theta = (\theta_1, \theta_2, \theta_3, \theta_4, \theta_5, \theta_6)$:

265
$$G_{controller}(s) = \frac{\theta_1 s^2 + \theta_2 s + \theta_3}{s^3 + \theta_4 s^2 + \theta_5 s + \theta_6} \tag{16}$$

Design objectives $(J_i(\theta))$ have to be quantities that the designer wishes to minimize. For the robust control benchmark, six functions that supply specification values for controller design will be used (also used in [15] and [18]):

- $J_1(\theta)$: Robust stability and robust performances $(Re(\lambda)_{max})$.
- $J_2(\theta)$: Maximum control effort (u_{max}).
- $J_3(\theta)$: Worst case settling time (t_{est}^{max})
- $J_4(\theta)$: Noise sensitivity $(noise_{max})$.
- $J_5(\theta)$: Nominal control effort (u_{nom}).
- $J_6(\theta)$: Nominal settling time (t_{est}^{nom})

To prevent instability problems when nominal or worst case poles are unstable:

- Nominal control effort and settling time $(J_5(\theta)$ and $J_6(\theta))$ are coerced to ∞.
- Maximum control effort $(J_2(\theta))$, the worst case settling time $(J_3(\theta))$ and noise sensitivity $(J_4(\theta))$ are coerced to ∞.

4.2   Graphical analysis of Pareto front

With the multiobjective evolutionary algorithm ε-MOGA [10] a Pareto front approximation of 2328 points is obtained[7]. Visual representation of the approximations of the Pareto front and the Pareto set is shown in figures 10, 11 and 12. These figures show the *Level Diagrams* method with Euclidean norm, 1-norm and ∞-norm respectively.

---

[7] An imposed designer constraint is that the search range for each parameter is limited to $\theta_i \in [-10, 25]$. To obtain this solution, the algorithm has made 52100 evaluations of objective vectors.

19

As can be seen, the volume of data hinders graphical analysis. Parallel coordinates, or scattered plots, are inadequate for this case. However, with the new representation method some valuable information can be interpreted.

Using *Level Diagrams*[8] the nearest zone to the ideal point of the Pareto front can be approximately established (table 1). It is worth remarking that the values differ depending on the norm used. For a geometrical interpretation, the Euclidean norm gives a better representation. The other norms give useful information for the decision-maker and depend on the preferences. It is recommendable to represent the same Pareto front with different norms to see the differences. Usually for DM purposes, it is sufficient to plot with the ∞-norm - as can be seen in the following analysis.

Using the Euclidean norm (figure 10), the lowest value is always over 0.9, and that means the Pareto front is relatively far from the ideal point. A sign of probable nonconvexity is that all Pareto points are above the hyperspheres of the 0.9 radius and below 1.75. Remember, that all objectives are normalized and the best value for a single objective is 0 and the worst is 1, meaning all points with a euclidean norm of 1 are on the hypersphere surface of radius 1. This hypersphere is nonconvex, and so it is certain that points above this hypersphere correspond to points of nonconvex zones of the Pareto front. Another sign of possible nonconvexity can be seen at J_4, where the nearest zone is horizontal and this means all these points have the same Euclidean distance (they are part of a hypersphere) so producing a nonconvex zone.

---

[8] A more accurate, even an exact, position of the nearest zone to the ideal point can be achieved by increasing the zoom ratio in the Level Diagrams, but this paper only intends showing how a DM could use the method in an easy and intuitive way.

Table 1

Values of objectives and parameter for the nearest points to the ideal.

i	1	2	3	4	5	6
	Values with Euclidean norm					
J_i	$[-0.03, -0.01]$	$[0.15, 0.22]$	≈ 80	$[0.5, 4]$	$[0.12, 0.2]$	≈ 80
θ_i	$[-5, -0.5]$	$[3, 5]$	≈ 0.15	$[16, 24]$	$[12, 25]$	$[14, 21]$
	Values with 1-norm					
J_i	≈ -0.015	≈ 0.17	≈ 90	≈ 0.1	≈ 0.12	≈ 70
θ_i	≈ -0.2	$[3, 4]$	≈ 0.15	$[22, 24]$	$[12, 18]$	$[15, 18]$
	Values with ∞-norm					
J_i	≈ -0.45	≈ 0.3	≈ 60	≈ 5	≈ 0.25	≈ 50
θ_i	≈ -5	≈ 6	≈ 0.4	≈ 17.5	≈ 20.5	≈ 19

308 A quick analysis of design parameters shows that parameter θ_5 easily reaches
309 its highest limit of 25. Therefore, good solutions can probably be found by
310 increasing this range. For the other parameters, it is possible to better adjust
311 the range of values for a new Pareto front search. For instance, all of the
312 parameters (except θ_1) are positive.

313 With 1-norm *Level Diagrams* (figure 11) it is possible to see indices of noncon-
314 vexity of the Pareto front. In the example, it is easy to see that lower values
315 of 1-norm are near the extremes of the Pareto front: the lower 1-norm value
316 of J_1 is near its worst value, and for J_2, J_3, J_4, J_5 and J_6 the lower 1-norm
317 values are near the low J_i $(i = 2, \ldots, 6)$ value.

318 ∞-norm *Level Diagrams* (figure 12) better show the worst objective - and give
319 a quick view of the weakness of each solution. It is usual to see V layouts
320 in several of the objectives, when an objective increases then others must
321 decrease. For this problem, the vertices of the V (the nearest point to ideal)
322 at objective J_1, J_2, J_4 and J_5 are around 50% of the scale of each function.
323 For J_3 and J_6 the points are mostly concentrated under values of 150 units.
324 That means these values are easily attainable - independently of the values of
325 the other objectives.

326 It can also be seen with all the norms that there are no important discontinu-
327 ities in any of the objectives. Reachable ranges for all objectives include the
328 complete range of the Pareto front (see axes X). This tells the designer (DM)
329 the order of magnitude that the objectives can achieve.

330 An interesting remark can be made for table 1: the nearest values with each
331 norm are quite different, this is due to the nonconvexity (with a convex Pareto,
332 the results are more similar). For instance, by comparing the Euclidean norm
333 and ∞-norm it is clear that the geometrical proximity to the ideal point (mea-
334 sured with the Euclidean norm) is not the best choice from the trade-off point
335 of view (measured with ∞-norm).

336 Generally, a nonconvex Pareto front and, in particular, a Pareto front, which
337 is far from the ideal point, represents a challenging problem for the DM.
338 It is difficult to select a single solution because there is not a clear trade-
339 off solution - and so the DM has to select according to his preferences and
340 experience. Therefore, ∞-norm *Level diagrams* offer better alternatives for
341 these problems.

342 In summary, a quick intuitive and quantitative approach to the performance

attainable with the solution of the Pareto front can be made with this graphical representation. To extract more quantitative information, these diagrams can be zoomed and coloured according to designer preferences - as shown in the following sections.

4.3 Including design preferences

To conclude with a specific solution, the designer or decision-maker (DM) has to establish a set of preferences. As a default, it is possible to select points nearest the ideal, but it may be that this is not the preferred solution.

As mentioned in the motivation section, different approaches to introducing preferences can be found in the literature. The *Level Diagrams* can be used in a posteriori and progressive methodology. This graphical representation, combined with a colouring methodology of the points based on preference, can be a powerful tool to help the DM make a decision.

The benchmark problem [28] established a specific requirement:

- The maximum settling time for the nominal system ($m_1 = m_2 = k = 1$) must be 15 seconds for unit impulse in perturbation w at time $t = 0$.

This constraint is translated to the objectives as $J_6(\theta) < 15\,sec$. The points that satisfy the constraints are coloured in dark red (figure 13, J_6 diagram has been zoomed between 11 and 40 to highlight zones of interest). It is now easier for the DM to choose an adequate solution. Among these points, a good choice is the point associated with the lowest norm, that is, the nearest one to the ideal point, for instance, if ∞-norm is preferred (see worst performance)

the solution is (see squared point at figure 13):

$$J_1 = -0.04855; \ J_2 = 0.449; \ J_3 = 21.9;$$
$$J_4 = 4.57; \ J_5 = 0.348; \ J_6 = 14.9;$$
$$\theta_1 = -4.643; \ \theta_2 = 9.57347; \ \theta_3 = 1.49719;$$
$$\theta_4 = 18.7568; \ \theta_5 = 22.7352; \ \theta_6 = 17.7596$$

(17)

Table 2

Preferences for the controller design.

	J_i^{HD}	J_i^{D}	J_i^{T}	J_i^{U}	J_i^{HU}	
J_1	-0.01	-0.005	-0.001	-0.0005	-0.0001	$Re(\lambda)_{max}$
J_2	0.85	0.90	1	1.5	2	u_{max}
J_3	14	16	18	21	25	t_{est}^{max}
J_4	0.5	0.9	1.2	1.4	1.5	$noise_{max}$
J_5	0.5	0.7	1	1.5	2	u_{nom}
J_6	10	11	12	14	15	t_{est}^{nom}

More sophisticated preferences can be considered, a good and intuitive way to set preferences is the idea proposed by Messac [16] with the range of preferences and the type of optimization to perform (see original source for more information).

In this problem, all objectives have to be minimized and the ranges of preferences can be established as shown in table 2. The designer has to choose the values J_i^x to define the ranges for each objective according to the following classification:

• Highly desirable (HD): $J_i \leq J_i^{HD}$

24

- Desirable (D): $J_i^{HD} < J_i \leq J_i^D$

- Tolerable (T): $J_i^D < J_i \leq J_i^T$

- Undesirable (U): $J_i^T < J_i \leq J_i^U$

- Highly undesirable (HU): $J_i^U < J_i \leq J_i^{HU}$

- Unacceptable (UNA): $J_i > J_i^{HU}$

With the table of preferences, it is possible to classify each point of the Pareto set according to designer preferences. For example, with table 2, a point is classified as follows:

$$
\begin{aligned}
J(\theta) &= (-0.0032, 0.95, 22, 0.4, 2.1, 14.5) \\
&\downarrow \\
&(D, T, HU, HD, UNA, HU)
\end{aligned}
\tag{18}
$$

A scoring system has to be established to colour *Level diagrams* according to this classification. The proposed system follows the 'ones vs others' criteria [9] rule (OVO rule) established by Messac [16]:

Full reduction for one criterion across a given region is preferred over full reduction for all the other criteria across the next best region.

In other words: (U, U, U, U, U, U) is preferred over (T, T, T, T, T, HU). A possible scoring system follows below:

- A vector of scores is generated (**score**), and each position of the vector corresponds to the score for each range of preferences. For the example of the six ranges (HD, D, T, U, HU and UNA):

$$
\mathbf{score} = (score_{HD}, score_D, score_T, score_U, score_{HU}, score_{UNA})
$$

---

[9] *criterion* is equivalent to *objective*

- An initial value is assigned for the two first preference ranges:

  · **score**$(0) = score_{HD} = 0$

  · **score**$(1) = score_D = 1$

- The following ranges are scored as follows, for $i = 2 \ldots Nobj - 1$ ($Nobj$ is the number of objectives):

$$\mathbf{score}(i) = Nobj * \mathbf{score}(i-1) + 1$$

Then, for the example with six ranges of preferences, the score vector is:

$$\mathbf{score} = (0, 1, 7, 43, 259, 1555)$$

A point A with (U, U, U, U, U, U) has a total score of $6 * score_U = 258$ and a point B with (T, T, T, T, T, HU) has a total score of $5*score_T + score_{HU} = 294$. As lower scores are better, so point A has a better score than point B satisfying the OVO rule.

Once the score system is established, the colour for the *Level diagrams* is assigned according to the score of each point. Then for the six-dimensional problem, if the preferences are those defined in table 2, the resulting coloured *Level Diagrams* are shown in figure 14. A darker colour means a lower score and so a better point. The DM can now choose one of the darker points, for instance, the point with the lowest norm (squared point at figure 14).

5 Conclusions

A new alternative visualization methodology for Pareto front representation is presented and called *Level Diagrams*. It enables analysis of large sets of a

26

high dimensional Pareto fronts and sets. The fundamental idea is classification by layers, and synchronous representation of all objectives and parameters. It is shown that this *Level Diagrams* representation enables a good analysis of the Pareto front, and so provides an excellent tool to help decision-making. In this article, only some of the Pareto front characteristics have been evaluated (discontinuities, closeness to ideal point, ranges of attainable values), but it already offers valuable information and seems to be open to other characteristic evaluations. New possibilities for incorporating designer preferences in this representation have been developed (based on scoring and colouring points of *Level Diagrams*) and will contribute to improving decision-making tools for multiobjective problems.

Acknowledgments

References

[1] G. Agrawal, C.L. Bloebaum, and K. Lewis. Intuitive design selection using visualized n-dimensional pareto frontier. In *46th AIAA /ASME /ASCE /AHS /ASC Structures, Structural Dynamics and MaterialsConference*, Austin, Texas, 2005.

[2] ATKOSoft. Survey of visualization methods and software tools, 1997.

[3] X. Blasco, J.M. Herrero, J. Sanchis, and M. Martínez. Decision making graphical tool for multiobjective optimization problems. *Lecture Notes in Computer*

428   *Science*, 4527:568–577, 2007.

[4] C.A. Coello Coello. Handling preferences in evolutionary multiobjective
430   optimization: A survey. In *IEEE Congress on Evolutionary Computation*, 2000.

[5] K. Deb. *Multi-Objective Optimization using Evolutionary Algorithms*. Wiley,
432   NY, 2001.

[6] Christian Fonteix, Silvère Massebeuf, Fernand Pla, and Laszlo Nandor Kiss.
434   Multicriteria optimization of an emulsion polymerization process. *European
435   Journal of Operational Research*, 153:350–359, 2004.

[7] Haley Halsall-Whitney and Jules Thibault. Multi-objective optimization for
437   chemical processes and controller design: Approximating and classifiying the
438   pareto domain. *Computers and Chemical Engineering*, 30:1155–1168, 2006.

[8] J.M. Herrero, M. Martínez, J. Sanchis, and X. Blasco. Well-distributed pareto
440   front by using the ε-MOGA evolutionary algorithm. *Lecture Notes in Computer
441   Science*, 4507:292–299, 2007.

[9] Juan Manuel Herrero. *Non-linear robust identification using evolutionary
443   algorithms*. PhD thesis, Universidad Politécnica de Valencia, Valencia, Spain,
444   2006.

[10] Juan Manuel Herrero, Xavier Blasco, Miguel A. Martínez, and Javier Sanchis.
446   Identificación robusta de un proceso biomédico mediante algoritmos evolutivos.
447   *Revista Iberoamericana de Automática e Informática Industrial*, 3:75–86, 2006.

[11] Chen-Hung Huang and C.L. Bloebaum. Visualization as a solution aid
449   for multi-objective concurrent subspaceoptimization in a multidisciplinary
450   design environment. In *10th AIAA/ISSMO Multidisciplinary Analysis and
451   Optimization Conference*, Albany, New York, 2004.

[12] Cengiz Kahraman, Da Ruan, and Ibrahim Dogan. Fuzzy group decision-making
453   for facility location selection. *Information Sciences*, 157:135–153, 2003.

[13] Paul J. Lewi, Jul Van Hoof, and Peter Boey. Multicriteria decision making using pareto optimality and PROMETHEE preference ranking. *Chemometrics and Intelligent Laboratory Systems*, 16(2):139–144, 1992.

[14] M. Martínez, J. Sanchis, and X. Blasco. Global and well-distributed pareto frontier by modified normalized normalconstraint methods for bicriterion problems. *Structural and Multidisciplinary Optimization*, 34:197 – 207, 2006.

[15] Miguel Martínez, Javier Sanchis, and Xavier Blasco. Multiobjective controller design handling human preferences. *Engineering Applications of Artificial Intelligence*, 19(8):927–938, December 2006.

[16] A. Messac. Physical programming: effective optimitation for computational design. *AIAA Journal*, 34(1):149–158, January 1996.

[17] A. Messac and C. A. Mattson. Generating well-distributed sets of pareto points for engineering designusing physical programming. *Optimization and Engineering*, 3:431–450, December 2002.

[18] A. Messac and B. H. Wilson. Physical programming for computational control. *AIAA Journal*, 36(1):219–226, February 1999.

[19] Kaisa M. Miettinen. *Nonlinear multiobjective optimization.* International series in operation research and management science. Kluwer Academic Publisher, 1998.

[20] M.Laumanns, L. Thiele, K. Deb, and E. Zitzler. Combining convergence and diversity in evolutionary multi-objective optimization. *Evolutionary Computation*, 10(3):263–282, 2002.

[21] Lionel Muniglia, Laszlo Nandor Kiss, Christian Fonteix, and Ivan Marc. Multicriteria optimization of a single-cell oil production. *European Journal of Operational Research*, 153:360–369, 2004.

29

[22] I.S.J. Packham, M.Y. Rafiq, M.F. Borthwick, and S.L. Denham. Interactive visualisation for decision support and evaluation of robustnes - in theory and in practice. *Advanced Engineering Informatics*, 19:263–280, 2005.

[23] Roberta O. Parreiras, João H. R. D. Maciel, and João A. Vasconcelos. The a posteriori decision in multiobjective optimization problems with Smarts, Promethee II, and a fuzzy algorithm. *IEEE Transactions on Magnetics*, 42:1139–1142, 2006.

[24] Andy Pryke, Sanaz Mostaghim, and Alireza Nazemi. Heatmap visualization of population based multi objective algorithms. *Lecture Notes in Computer Science*, 4403:361–375, 2007.

[25] L. Rachmawati and D. Srinivasan. Preference incorporation in multiobjective evolutionary algorithms: a survey. In *IEEE Congress on Evolutionary Computation*, 2006.

[26] J. Renaud, J. Thibault, R. Lanouette, L.N. Kiss, K. Zaras, and C. Fonteix. Comparison of two multicriteria decision aid methods: Net flow and rough set methods in a high yield pulping process. *European Journal of Operational Research*, 177:1418–1432, 2007.

[27] Yee Swian Tan and Niall M. Fraser. The modified star graph and the petal diagram: Two new visual aids for discretealternative multicriteria decision making. *Journal of Multi-Criteria Decision Analysis*, 7:20–33, 1998.

[28] B. Wie and D. Bernstein. Benchmark problems for robust control design. *Journal of Guidance, Control and Dynamics*, 15(5):1057–1059, September 1992.
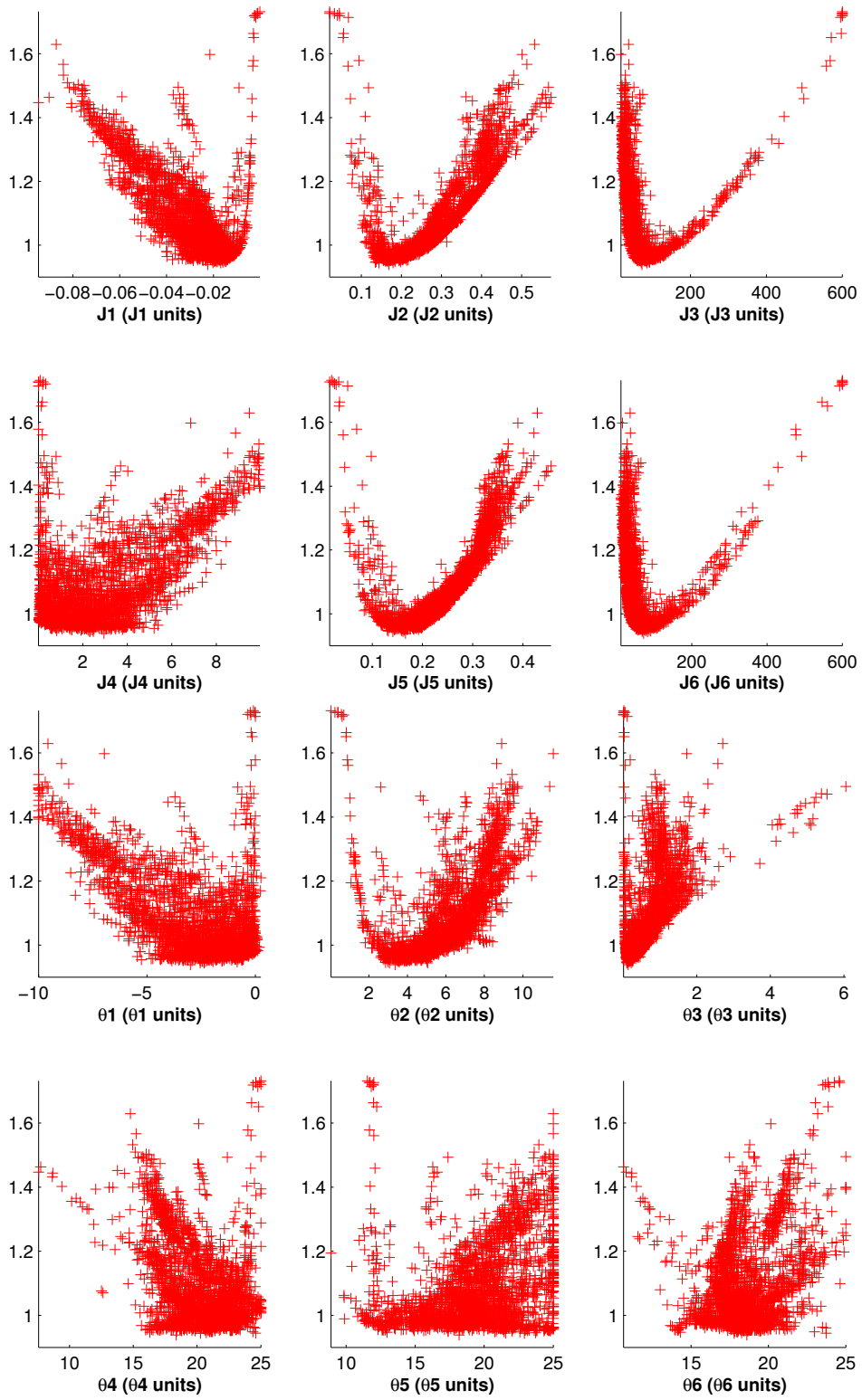
30

Fig. 10. Euclidean norm *Level Diagrams* representation of the approximation of the Pareto front and set for the benchmark problem.
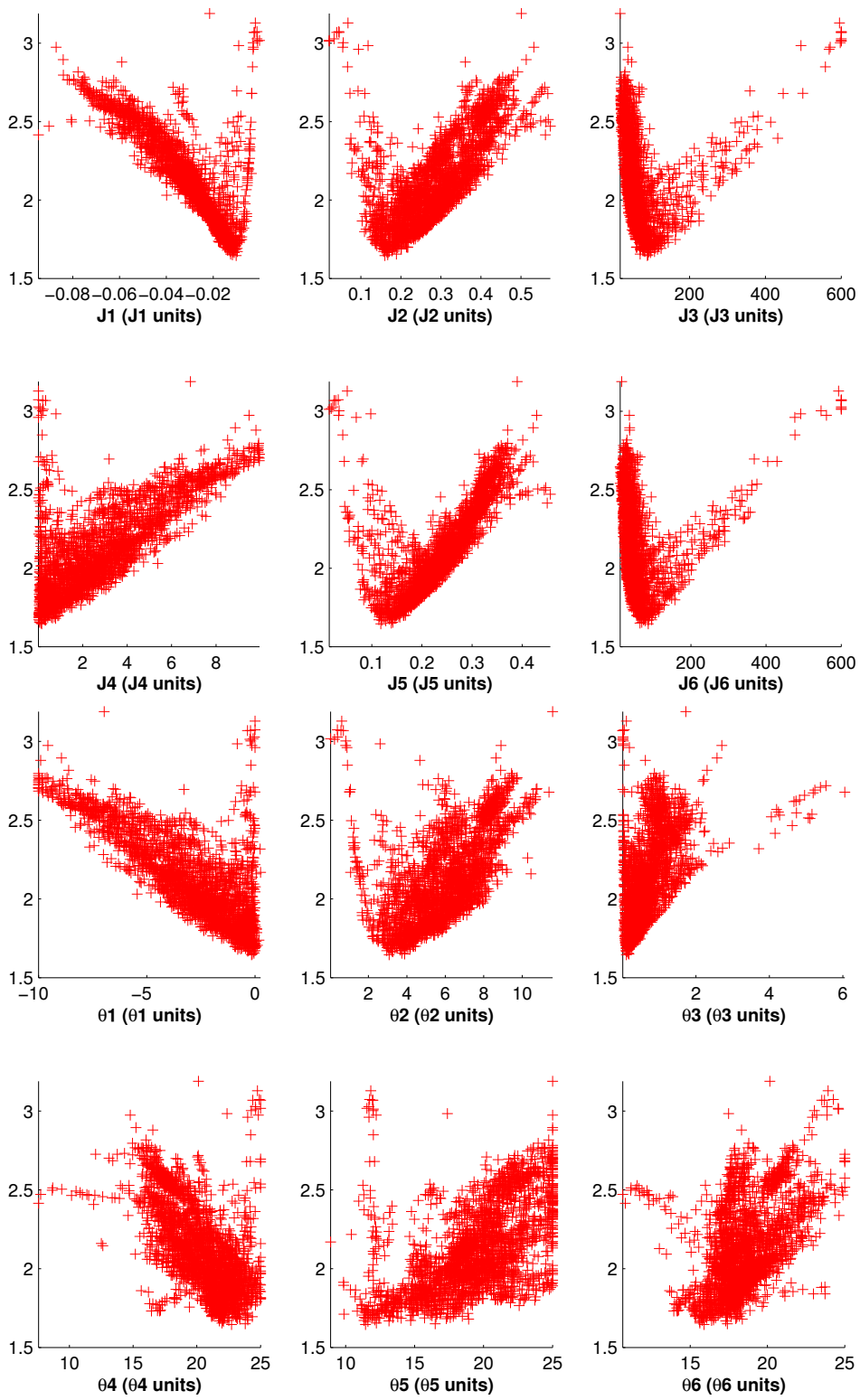
31

Fig. 11. 1-norm *Level Diagrams* representation of the approximation of the Pareto front and set for the benchmark problem.

Fig. 12. ∞-norm *Level Diagrams* representation of the approximation of the Pareto front and set for the benchmark problem.
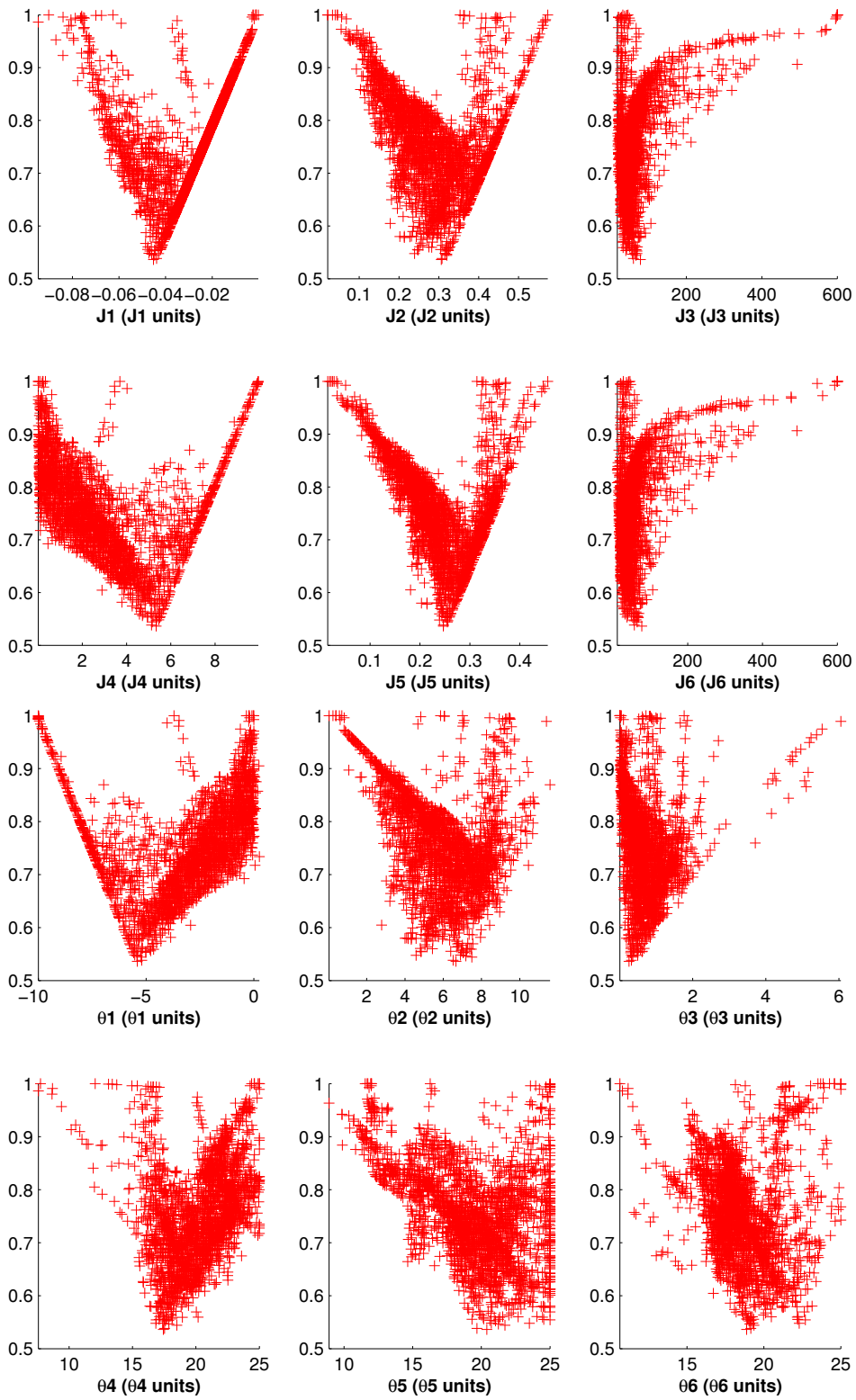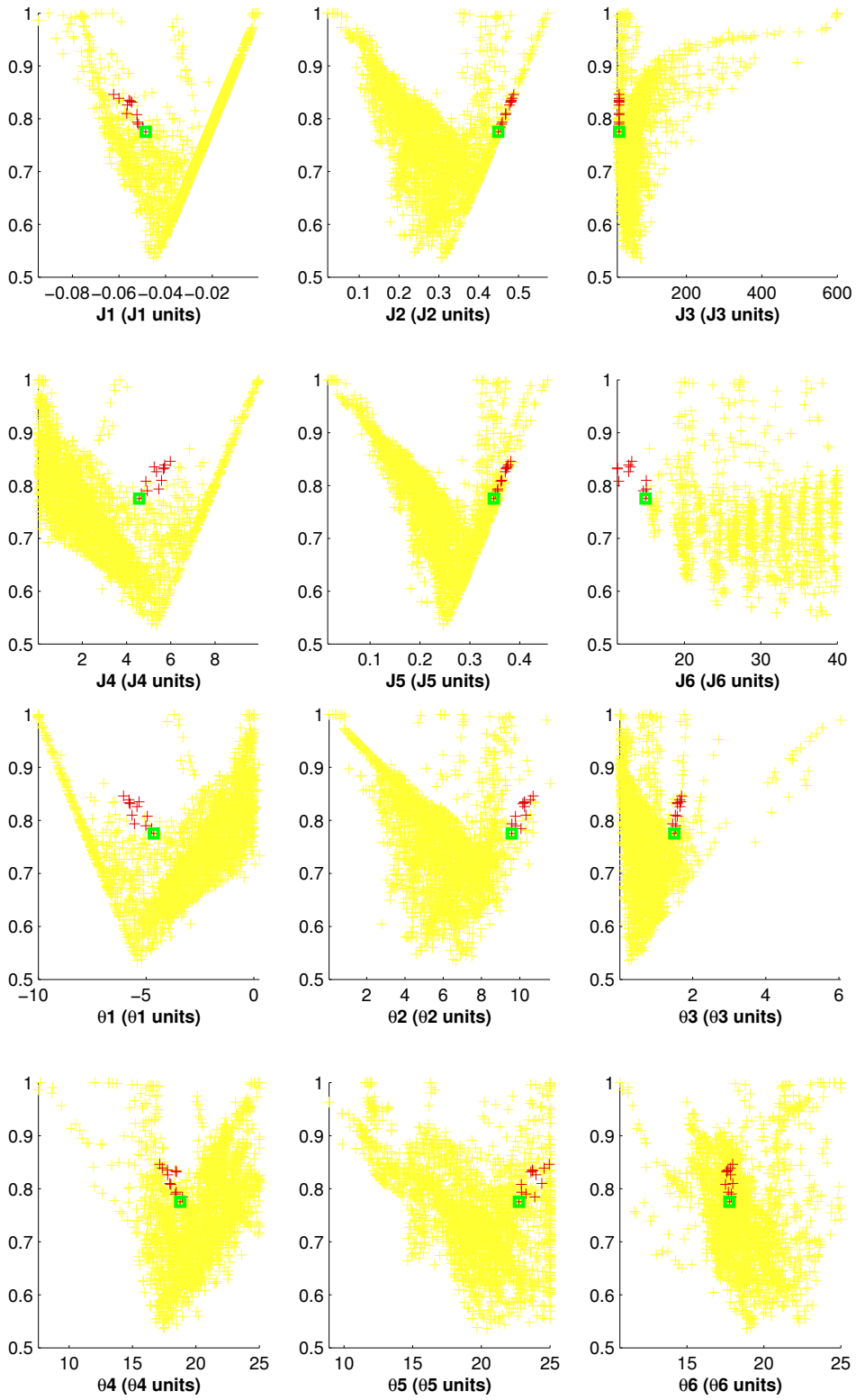
33

Fig. 13. ∞-norm *Level Diagrams* representation of the Pareto front and set for the benchmark problem. Points that satisfy $J_6 < 15\,sec$ are coloured in red (dark colour). The selected point is squared. J_6 diagram has been zoomed between 11 and 40.
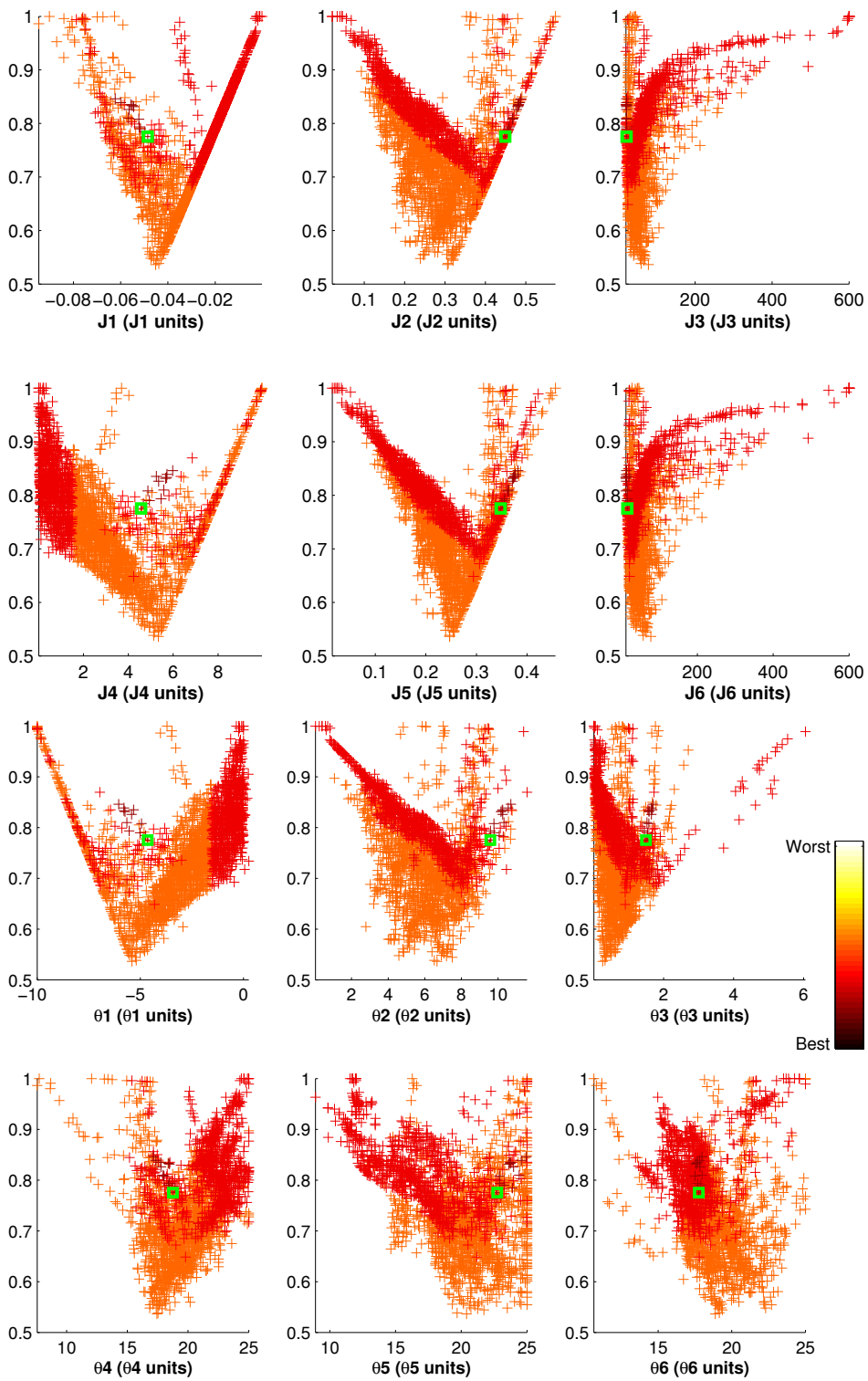
34

Fig. 14. Coloured ∞-norm *Level Diagrams* representation of the Pareto front and set for the benchmark problem. Better points in darker colour. The selected point (darker with lower norm) is marked with a square.